

THE INSTRUMENTED FRISBEE^(R) AS A PROTOTYPE FOR PLANETARY ENTRY PROBES

Ralph D Lorenz^(1,2)

⁽¹⁾Lunar and Planetary Lab, University of Arizona, Tucson, AZ 85721-0092, USA email: rlorenz@lpl.arizona.edu

⁽²⁾Planetary Science Research Institute, The Open University, Milton Keynes, UK

ABSTRACT

A Frisbee has been equipped with sensors, batteries and microcontrollers for data acquisition to record its translational accelerations and attitude motion. The experiments explore the capabilities and limitations of sensors on a rapidly-rotating platform moving in air, and illustrate several of the complex gyrodynamic aspects of frisbee flight. The experiments constitute an instructive exercise in aerospace vehicle systems integration and in attitude reconstruction.

1. INTRODUCTION

A remarkable feature of the flight of spin-stabilised disc-wings (most familiar in a recreational form such as the 'Frisbee', a trade-mark of Wham-O, Inc.) is that a wide range of nonmonotonic flight behaviours may be generated by manipulating the launch conditions (launch speed and elevation, angle of attack, and spin rate.) These are a result of the combined gyrodynamic and aerodynamic properties of the disc [e.g. 1,2].

The aerodynamic properties of flying discs have been studied in wind tunnel tests with a disc mounted on a motorized [3]. This work (see also [4]) has shown how the pitch moment coefficient, as well as the roll and sideforce coefficients, vary as the advance ratio increases to around unity. Note that the lift and drag coefficients are relatively insensitive to spin.

In recreational applications, a frisbee may routinely fly at angles of attack up to 90° in a conventional throw, and indeed up to -90° in throws such as the 'hammer' where the disc is thrown at a slightly negative angle of attack, to roll onto its back and descend near-vertically in an inverted attitude.

In order to explore these flight regimes and to investigate the capabilities of on-board measurements, we have undertaken experiments with free-flying discs equipped with on-board sensors and data acquisition equipment.

An additional motivation for these tests is the evaluation of attitude and trajectory determination methods for planetary probes. These, such as the Mars

Pathfinder probe or the Huygens probe to Titan, are spun for attitude stability. Their dynamics are inferred from the data telemetered from a small number of sensors such as gyros and accelerometers to determine the vehicle's flight path, and to infer the density of the atmosphere from the aerodynamic deceleration in flight. Since the measured deceleration relates directly to both the atmospheric density and to the drag coefficient, it is vital for accurate atmospheric measurements that the drag coefficients as a function of angle of attack be known, and the angle of attack history be known.



Figure 1. Test site and launch configuration. Note the high angle of attack of the disc.

Disc-wings have also been proposed as an architecture [4] for Unmanned Aerial Vehicles (UAVs) - onboard sensing will be necessary to implement guidance and control on such vehicles.

2. INITIAL EXPERIMENTS

A commercial (175g 'Wham-O Competition Frisbee') disk was obtained for tests. Initial experiments used an Analog Devices ADXL202 two-axis accelerometer, with its pulse-width modulated digital data sampled and stored by a Parallax Inc., Basic Stamp 2 microcontroller (BS2IC). $\sim 6\text{mA}$. At 6mA this could be powered by small Lithium 'button' cells (model CR2032). The two accelerometer axes were mounted along and orthogonal to the axis of the disk and were calibrated simply by holding the disc with the sensitive axes along against the local gravity vector.

The microcontroller was programmed in Basic to sample and store the two accelerometer axes, as an 8-bit number (representing from +2 to -2g) into the 2K on-board EEPROM at about 65 sample pairs/sec. We have used similar equipment to measure swing dynamics of parachute-borne instrument packages [5].

The microcontroller and accelerometer were attached with silicone adhesive to the underside of the frisbee (see fig.2), with the accelerometer mounted close to the center of the disk. The batteries were similarly mounted close to the other items to minimize any displacement of the center of mass or change in moments of inertia. The equipment had a mass of about 28g, giving a flying weight of 204g. Further particulars of the construction, and code available for download, have been published in the electronics literature [6.] More serious weight-reduction efforts, e.g. use of surface-mount components, could reduce the instrumentation mass by factor of 2-3, although at the expense of considerable labor.

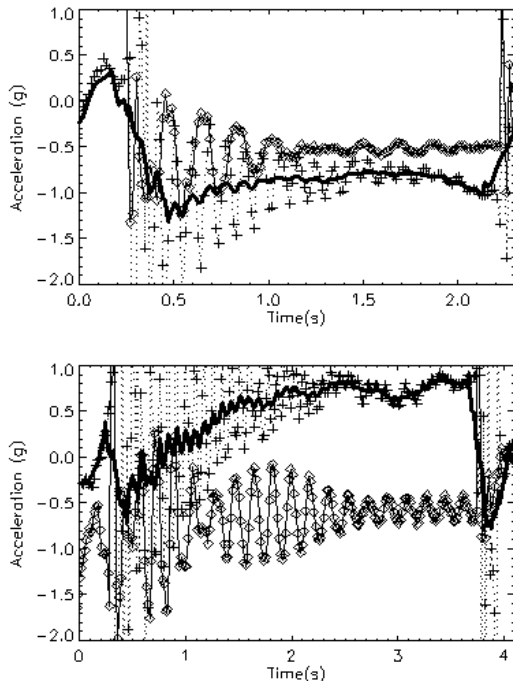


Figure 2. Results from 1st generation disc. Radial (solid/diamonds) and axial (dotted/crosses with smoothed thick line) acceleration. Top - conventional level throw. Note the offset in radial acceleration (due to centripetal acceleration off-center) and the spin modulation. Radial accelerometer shows damped $2x/\text{period}$ modulation due to nutation. Bottom - 'Hammer' throw, where disc is thrown in vertical orientation and rolls onto its back due to the large pitch moment at negative angles of attack -- hence axial signal of $\sim +1g$ during later part of flight. Note radial signal vanishes at $\sim 1s$ -- see fig 13.

Flow disturbance was minimized by fairing the equipment with adhesive tape, to present a smooth profile. Since wind-tunnel tests show that the pressure on the underside of a disk is modest and uniform, it is believed that the instrumentation's perturbation to the aerodynamic characteristics is minimal.

3. SECOND AND THIRD GENERATION TESTS

A second, more elaborate set of instrumentation was developed in early 2004 (figure 2). This used a more powerful microcontroller. The Netmedia Inc., BX-24 microcontroller is a device with 32,000 bytes of EEPROM for program and data storage, with 8 on-board 10-bit analog-to-digital converters, also programmable in a Basic programming language. The BX-24 required a power source with higher current than CR2032 button cells could provide. We used a string of 6 1/3-AAA Nickel Metal Hydride cells giving 7.2V . These cells were mounted along the inside of the rim of the disc.

Components were mounted using a glue gun, usually in holes or recesses cut with rotary tools both to maximize the security of their attachment (discs tend to be made of high-density polyethylene or polypropylene to which adhesives do not bond well), to minimize the projection of components into the airflow and to minimize the change in weight and moment of inertia introduced by their installation.

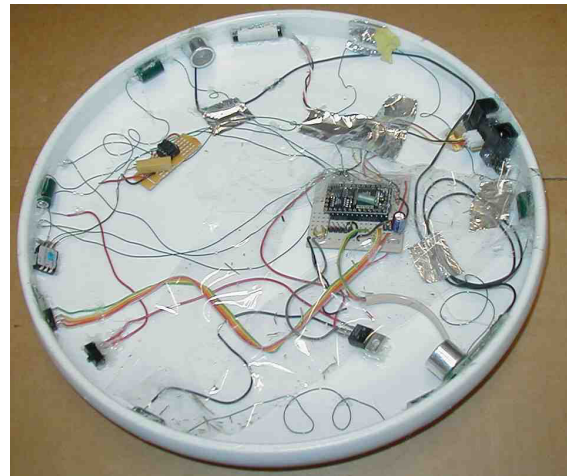


Figure 3. 2nd Generation Frisbee showing equipment mounted on underside.

This second-generation disc employed ADXL202 accelerometers as before (this case mounted on the rim of the disc, rather than projecting up from its centre.) Two sun sensors, photodiodes yielding a current with a roughly cosine response to sun angle were mounted, one roughly flat on the upper side of the disc, the other on a steeply angled part of the rim. During early

Tucson summer, the sky is persistently clear and thus sun sensors yield excellent signals.

The magnetometers are small, cylindrical fluxgate units (FGM-1) sold for mobile robotics. They provide a 5V square wave pulse with a period proportional to the field along the sensitive axis. One was mounted tangentially inside the rim of the disc; the other was mounted radially, canted at 45 degrees to the disc axis.

Sensors tried on the 2nd generation disc also include a Sharp GP12A02 infrared range sensor (this projects a spot of IR onto a scene, and uses a position-sensitive detector to measure the spot position and thus determine the distance to the reflecting surface.) This sensor gives an analog voltage for distances between about 20cm and 80cm. Although some interpretable data was obtained, the somewhat uneven sensor output and low update rate (new distances are determined only 30 times per second) eroded the sensor's usefulness.

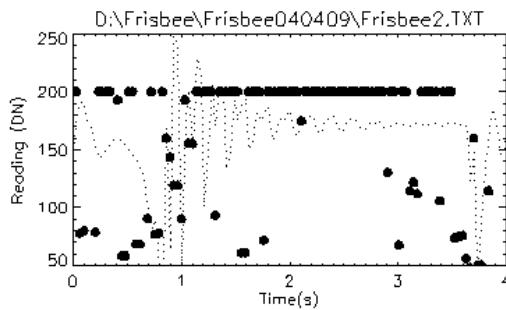


Figure 4. Radial acceleration (dotted line) and IR data (circles). Usable signal is only obtained at the beginning and end of the flight.

A small sonar unit (Devantech SRF-04) was modified to transmit an ultrasound pulse across the underside of the disc, in the hope of obtaining a spin-modulated time-of-flight measurement that might therefore indicate the mean airspeed across the underside of the disc. This was generally noisy, although did sometimes yield a perceptibly spin-modulated signal.

Finally, a Fujiwara XP150 pressure sensor was mounted on the curved rim. This is a differential pressure sensor with built-in temperature compensation and amplification giving a 0-4.25V output range for pressure differences of 150 Pa. For this application, the sensor output was amplified by a further factor of 30 in the hope of measuring directly the suction peak on the upper leading edge of the disc. A differential measurement is somewhat unsatisfactory in that the 'reference' pressure is that inside the lip on the underside of the disc, which itself changes during the rotation. Again, some notably spin-modulated signals were recovered, but not reliably.

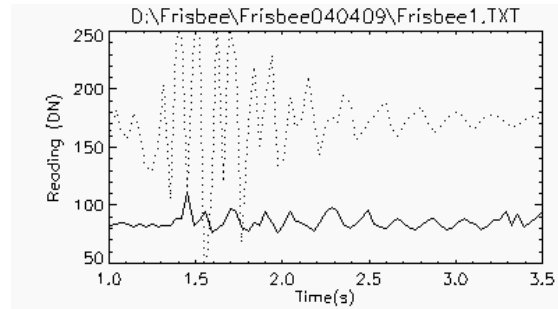


Figure 5. Axial acceleration (dotted line) and speed-of-sound 'anemometer': spin modulation suggests there is some flight speed information in the data.

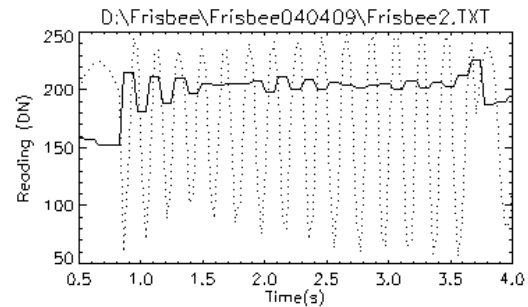


Figure 6. Magnetometer data (dotted line) showing constant amplitude and thus attitude over the last 1.5s of flight. Solid line is pressure sensor output - strongest immediately after release, and notably spin-modulated, as expected.

This 2nd generation testbed confirmed that the attitude sensors and the BX24 and battery installation were workable, even though they brought the instrumented disc mass up to 260g. It was noted that the large number of sensors, confronted with the fixed sampling throughput of the microcontroller, gave sampling rates slightly lower than ideal.

Thus the platform was modified into the 3rd generation disc, with which the principal results of this paper were obtained. This used fundamentally the same architecture, except with a second BX24 microcontroller running in parallel to double the data acquisition capability. A second FGM-1 magnetometer was added, as well as a second accelerometer. This two-axis device, an ADXL210, was mounted flat on the disc center. This device has a sensitivity somewhat low for flight measurements (it is identical to the ADXL202 but with a range of +/-10g) but permits the recording of the accelerations during the throw.

The sonar was modified with a down-looking sonar used as an acoustic altimeter. The device itself (SRF-08) is the same as the SRF-04 used in the time-of-flight

experiment, but with the incorporation of a dedicated microcontroller to perform timing. This allows the master processor (the BX24) to perform other duties during the altimetry measurement. Whereas the time-of-flight pulse took under a millisecond to cross the disc, in the altimetry application the waiting time would be prohibitive - at typical heights of 3m, the sound pulse takes some 18ms to return.

4. SENSOR CALIBRATION

Some analog signal processing was performed in hardware (e.g. resistor network on the sun sensors, amplifier for the pressure sensor.) Further processing was performed in software to yield an 8-bit number for each sensor to facilitate storage as a single byte.

The attitude sensors (sun sensors and magnetometers) were calibrated by mounting the frisbee on a motorized alt-azimuth mount (that of a Meade LX200 20cm telescope). Although the orientations were simply set manually with the motors turned off, this approach yielded a very stable, smooth mount for making measurements at a selection of attitudes. After aligning level and due north, the calibration attitudes were simply read off from the telescope setting circles. A 'lazy susan', a bearing table for presenting condiments in a kitchen, was attached to the mount and could be spun by hand.



Figure 7. Calibration arrangement.

Results are shown in figure 3. The signal processing was designed to yield an approximately cosine response with regard to sun (or field) direction. Between the peak and the trough of the reading, the orientation measurements may have a sensitivity of around 1 DN per degree (all measurements are

recorded and reported as 8 bit integer Data Numbers DN.)

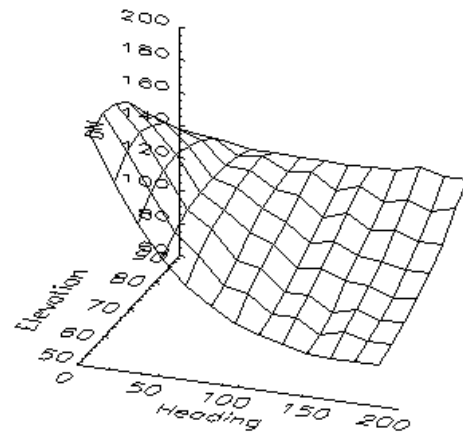
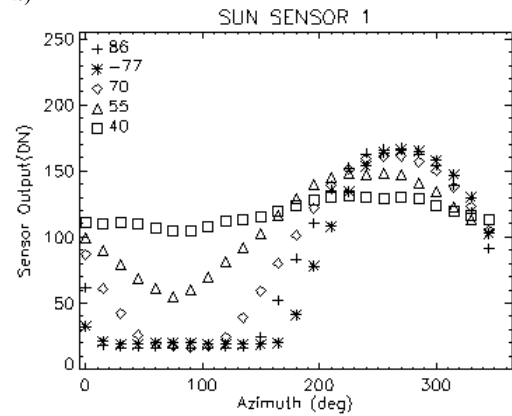


Figure 8. Example sensor calibration data. (a) shows sun sensor 1 output, with the disc attached to the telescope mount and not rotating. Various symbols correspond to different elevation angles (90 degrees is vertical) and the telescope (and spin axis) is rotated to different azimuths. (b) carpet plot of the minimum Magnetometer 1 output as the disc spins with the spin axis at various elevations and spin axis azimuths

5. RANGE INSTRUMENTATION

To determine aerodynamic coefficients, the flight conditions (specifically flight speed and flight path angle) must be known. These are difficult to obtain with on-board measurements, since GPS measurements are not practicable on such short flights, and so additional instrumentation is needed.

A video record from a conventional camcorder was digitized after the tests, and X-Y positions of the disc in the image plane were recorded for each frame to yield a record of the translational motion of the disc for most of its flight, in particular providing a launch speed and angle constraint. The image coordinates were

converted into physical distance using red cones placed in the field as fiducial markers every 2.5m. We note the work of Hummel [7,8], who has conducted free-flight measurements using a dedicated high-speed video system (120 and 200 frames per second), deriving aerodynamic coefficients (assumed to be smoothly-varying functions of angle of attack) from the trajectory data alone.

6. FLIGHT RESULTS

The video trajectory data for one flight (#4) is shown in figure 4. The characteristic 'airfoil' trajectory is observed, with a near-linear shallow upwards ramp before the disc has slowed appreciably, then a slow and steepening descent. The video record was obtained looking north, while the disc was thrown in an ESE direction. From the perspective of the thrower (not apparent in this video record) the disc curved slightly to the left (north) towards the end of its flight. Eastward distance was 22m, with a ~6m slide to the N.

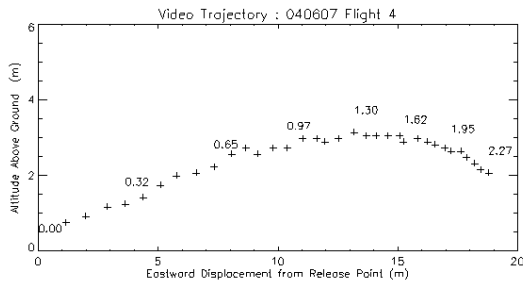


Figure 9. Frisbee trajectory from video record. (a) X-Y position, with time in seconds indicated along the trajectory.

Figure 10 shows the attitude sensor and accelerometer data from the same throw. Spin modulation on is seen on both magnetometers and sun sensors at ~6.5 Hz. Modulation envelope varies due to the slow precession of the spin axis during flight.

The accelerometers are over-ranged (span is +/-2g) at launch and impact. The radial accelerometer is spin-modulated as expected about its zero value of 170DN, though with some twice-per-rotation nutation signal just after launch. Hummel [8] has similarly observed nutation in the first second or so of frisbee flight - the nutation is caused by the angular momentum vector imparted by the thrower being misaligned with the axis of maximum moment of inertia. Energy dissipation, either by flexing of the disc, or by aerodynamic forces, tend to damp this nutation quickly. The Axial accelerometer shows spin modulation (coning) due to sensor misalignment with principal axis, about a near-constant flight signal of ~1.3g.

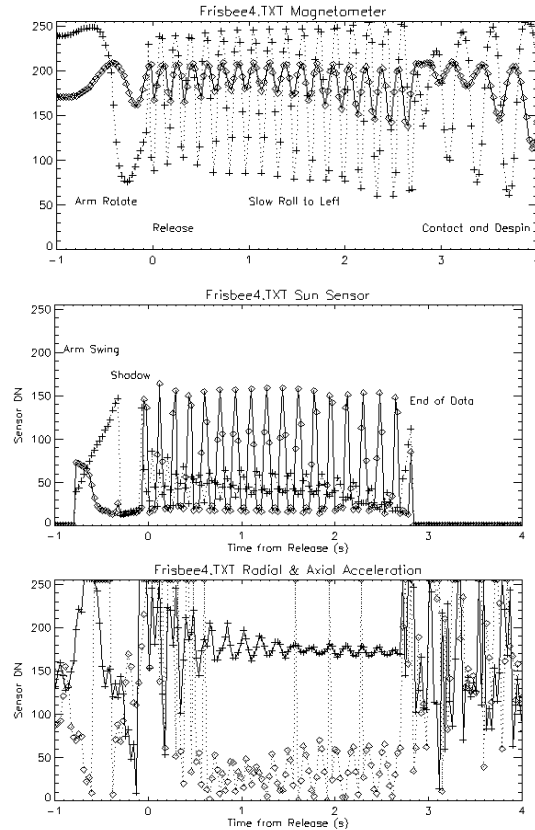


Figure 10. Data from dynamics sensors - same flight as figure 4. Magnetometer record (a) shows spin modulation on magnetometers 1 (dotted line/crosses) and 2 (solid line/diamonds) at ~6.5 Hz. Modulation envelope varies due to tilt of spin axis during flight. Sun sensors (b) show similar effects. Accelerometers (c) are over-ranged (span is +/-2g) at launch and impact. Radial accelerometer (solid line/crosses) is spin-modulated as expected about its zero value of 170DN, though with some twice-per-rotation nutation signal just after launch. Axial accelerometer (dotted line/diamonds, with zero level ~110) shows spin modulation (coning) due to sensor misalignment with principal axis, about a near-constant flight signal of ~1.3g.

Figure 6 zooms in on these parts of the acceleration signals, with a magnetometer overlain to indicate the spin phase. The accelerometers are particularly sensitive to nutation and coning effects, which are well-known in spacecraft engineering. Nutation is commonly observed in spinning satellite deployments due to slight tip-off errors on separation - Spencer et al. [9] show accelerometer data from the Mars Pathfinder entry probe with a nutation signal (although they incorrectly label it as 'coning'), and a nutation was generated on the Giotto spacecraft [10] by a dust

impact during its close approach to comet Halley in 1986.

7. ATTITUDE RECONSTRUCTION

The determination of the spin axis and phase of a rotating vehicle is of course a standard problem in spacecraft attitude dynamics, and a combination of sun sensor and magnetometer is often used (e.g. [11,12]) A spacecraft is likely to maintain a constant spin axis and rate over periods of weeks, and a variety of on-board filtering approaches are often used to estimate the attitude. A major difference here is that the spin axis of a frisbee in flight is being precessed rapidly.

Full exploitation of the data from frisbee flights with a fixed (rather than evolving and experimental) sensor configuration may be best accomplished with a forward model of the flight and attitude dynamics, which computes explicitly the expected signal from each of the sensors. By performing Euler rotations, the dot product of the magnetometers with the field vector, and that of the sun sensors with the solar vector, can be calculated at every instant of flight, and a sensor model applied to derive the corresponding stored data number. Expected acceleration signals can similarly be computed. Launch conditions and a model of the aerodynamic coefficients can be adjusted such that the model time series of the various sensors match those recorded.

For the present proof of concept, we employ a heuristic approach, wherein the envelope of the spin-modulated sensor data is used to define, by manual best fit to the data such as that in figure 3, the spin axis direction.

In this exercise, tests were performed quite deliberately in the morning around 8am, when the sun was sufficiently high above the horizon to give a good signal, but was still well in the East. Early afternoon tests would have suffered not only from more convectively unstable conditions with stronger winds, but the sun direction and magnetic field direction would then be approximately collinear, making the attitude determination degenerate.

Since mechanical construction was performed with hand tools and adhesives, without precision alignment fixtures, sensor orientation was determined by post-hoc measurement. As an example, sun sensor 2 was nominally mounted flat in the plane of the disc but after the mounting adhesive had a perceptible, but difficult to measure, inclination to the plane. Modest spin modulation is therefore evident in its flight data (e.g. at one point in flight 6, the reading varies 20-45 ; later the variation is 25-70). Both of these ranges (other data show the sensor to report approximately 20+130

$\cos(\Theta)$ where Θ is the angle between the sensor normal and the sun) are consistent with a mounting offset of 6 degrees.

For the flight shown in figures 4 and 5, the sensor data around 1s after release was best fit with an elevation of 70 degrees (i.e. spin axis was 20 degrees from vertical) and an azimuth of 120 degrees (i.e. the spin axis was tilted towards WNW). If the disc were flying horizontally in an ESE direction, it would therefore have a 20 degree angle of attack (see figure 8 for the relationship of the body sensor axes to lift and drag, and the definition of angle of attack and flight path angle.)

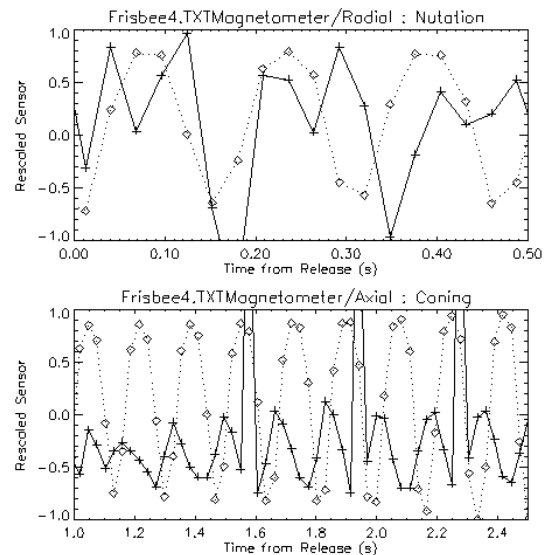


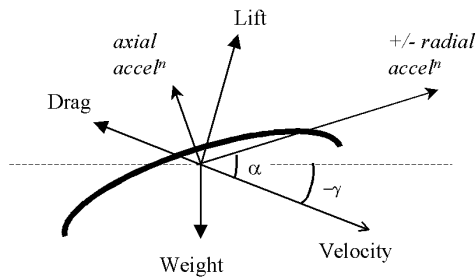
Figure 11. Nonideal dynamic signatures in the acceleration records (solid line/crosses), with magnetometer for spin-phase reference (dashed line/diamonds). (a) shows a nutation signature (~twice per spin period) in the radial acceleration early in the flight - compare with figure 5 later in the flight where this signature is damped out. (b) shows coning (once per spin period) in the axial accelerometer, indicating that the accelerometer is not truly aligned with the spin axis. The axial accelerometer also shows nutation early in the flight.

At ~2.5s, shortly before impact, the attitude has precessed due to the disc's pitch moment. The best-fit attitude has an elevation of 60 degrees and a heading of 150 degrees. This corresponds to a precession of about 14 degrees in total.

8. ACCELERATIONS

The acceleration recorded by the radial accelerometer is by design spin-modulated. The mean value is nominally zero, although sensor positioning and

orientation may introduce a centripetal acceleration component, with an amplitude related to the near-constant spin rate. While the modulation envelope is defined by the lift and drag forces, the phase of the peaks and troughs in the signal relative to the peaks and troughs in the attitude sensor record can be used to infer the projection of the flight direction in the spin plane, a useful parameter in guiding a disc wing via spin-phased actuators such as flaps.



α = Angle of Attack
 γ = Flight Path Angle

Figure 12. Forces on flying disc, and their measurement. Measurements are body-fixed, ideally along the spin axis and orthogonal to it (i.e. radial).

Note that the radial signal amplitude and phase is affected not only by the magnitude of the lift and drag, but also by the attitude (see figure 12) which controls how these two forces are projected into the spin plane and thus the radial sensing direction.

Figure 13 shows the radial accelerometer record towards the end of flight, with magnetometer 1 overlain as a phase reference. It can be seen that the acceleration peaks before the magnetometer, indicating a particular heading. However, within 4 spin periods (~0.6s) the phase reverses, with the acceleration peaking after the magnetometer. This does not indicate a 180 degree turn in flight, but rather the changing dominance of the two terms that contribute to the radial acceleration $(D\cos(\alpha)-L\sin(\alpha))/M$, where M is the mass of the disc (0.26kg) and other terms are defined in figure 12. Using the coefficients from [3] the net radial force coefficient $C_d\cos(\alpha)-C_l\sin(\alpha)$ can be calculated, and is shown in figure 13.

It is seen that this function has a maximum value at a modest angle of attack (~8 degrees, coincidentally close to the angle at which a disc has zero pitch moment, i.e. flies in trim.) Between 20 and 35 degrees, the function decreases rapidly and becomes negative. It is this change of sign that is responsible for the change in phase of the radial acceleration signal.

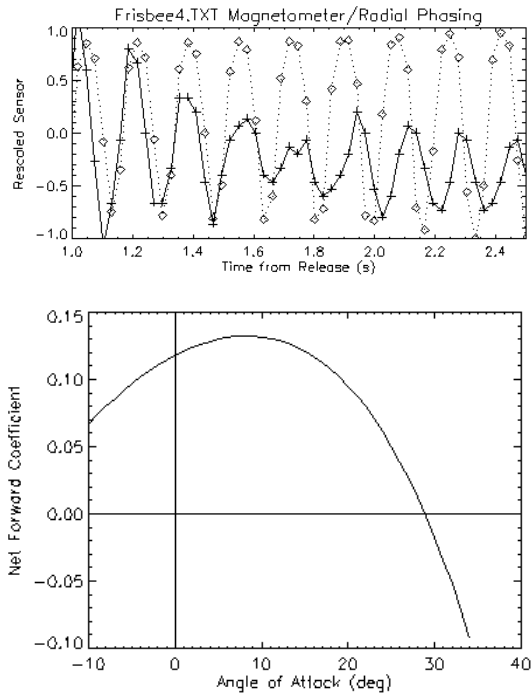


Figure 13. (a) The radial acceleration record (solid line/crosses) against the magnetometer record (dotted line/diamonds). Note that the acceleration initially peaks before the magnetometer, a phasing that could be used to determine the direction of flight. Within 4 spin periods (<1s) the phasing reverses, due to the swiftly-increasing angle of attack (b) The net forward radial component of lift and drag, $C_d\cos(\alpha)-C_l\sin(\alpha)$, using a quadratic and linear fit to C_d and C_l : at just under 30° , the net component is zero. Beyond 30° , the component is negative, and hence the phase of measured radial acceleration with respect to the forward direction is reversed.

The function is zero, corresponding to a vanishing of the radial signal, at a critical angle of attack of around 28 degrees. In principle, one can deduce from the radial acceleration record when the disc encounters this critical angle (though of course the value will depend on the actual variation of the coefficients with angle of attack - the plot shown is from only the linear and parabolic fits.)

9. AERODYNAMIC COEFFICIENTS

Knowing the disc mass properties, the flight speed and the attitude as a function of time, the aerodynamic coefficients can be produced – lift and drag from instantaneous accelerations resolved into the lift and drag directions., Moment coefficient measurement requires differencing between successive attitude determinations e.g. (fig 14.) to determine precession rates.

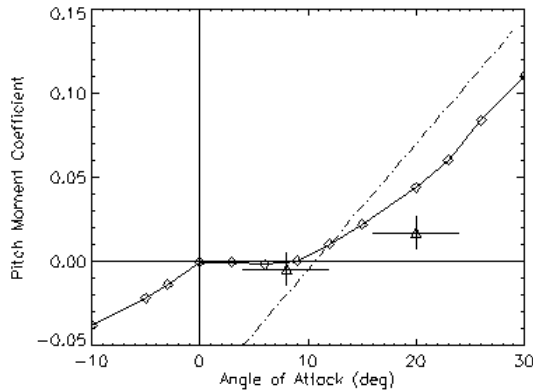


Figure 14. Pitch moment coefficient (diamond/solid line from [4], dot-dash line from [7]). Triangles from flight data in this paper.

10. CONCLUSIONS AND FUTURE WORK

This work has demonstrated that useful flight data on frisbee dynamics can be obtained with onboard instrumentation at rather modest effort and expense. Additional range instrumentation is required to document the flight velocity in order to recover aerodynamic coefficients : a conventional video camera has proven adequate.

A combination of magnetometer and sun sensor data can adequately constrain the attitude of the disc in flight. Sensor mounting offers some tradeoffs. Precise spin-axis alignment is difficult, especially since the equipment modifies the mass properties of the disc, whereas data reduction is simplest if both sensors are aligned with the spin axis. On the other hand, sensors mounted in the spin plane can provide spin-phase information. It has been easiest to mount sensors at an intermediate orientation, and recover the attitude by empirical fitting of sensor readings to data from known orientations.

Accelerometer data has generally been of good quality, although care sensor mounting position and orientation can improve the signal by suppressing coning and nutation sensitivity. Nonetheless, relatively simple algorithms can determine when a sensor is pointed in the forward direction during steady flight - allowing the actuation of control surfaces at a specific spin phase for manoeuvring. Similarly, the acceleration peaks relative to the attitude references can permit on-board determination of heading. A combination of these two may permit autonomous guided flight of disc-wings. An interesting recreational possibility might be a frisbee that homes in on, or attempts to avoid, a person.

Combined attitude information, accelerations, and speed documentation from the video record, allow recovery of aerodynamic coefficients. Our measurement of lift, drag and pitch moment coefficients are in agreement with published wind-tunnel measurements. The free-flight technique lends itself to application in conditions (e.g. high- α) that are challenging for wind-tunnels.

The ultrasonic sensors (speed of sound, and range) have not given encouraging results to date, perhaps as a result of turbulent conditions around the transducers. The infrared ranger gave similarly erratic results, perhaps largely due to its modest refresh rate (~25Hz) or poor performance in very bright conditions.

ACKNOWLEDGEMENTS

Jessica Dooley is thanked for assistance with the experiments and for digitizing the video record. The work was partly supported by Cassini.

REFERENCES

1. Bloomfield, L. A., The Flight of the Frisbee, Scientific American, p.132 April 1999
2. Lorenz R.D., Flying Saucers, New Scientist, 40-41, 19 June 2004
3. Potts, J.R. and W.J. Crowther, Frisbee Aerodynamics, AIAA-2002-3150, 20th AIAA Applied Aerodynamics Conference and Exhibit, 24-26 June 2002, St. Louis, Missouri.
4. Potts, J. R. and W. J. Crowther, Disc-Wing UAV: A Feasibility Study in Aerodynamics and Control, CEAS-AARC-2002.
5. Dooley, J. M. and R. D. Lorenz, A Miniature Probe-Parachute Dynamics Testbed, in Proceedings of the Workshop on Planetary Entry and Descent Trajectory Reconstruction and Science, Lisbon, Portugal October 2003 (published as ESA SP-544, European Space Agency, Noordwijk, the Netherlands)
6. Lorenz, R. D., Frisbee Black Box, Nuts and Volts Vol.25 No.2 (February 2004) pp.52-55
7. Hummel, S. and M. Hubbard, Identification of Frisbee Aerodynamic Coefficients using Flight Data, 4th International Conference on the Engineering of Sport, Kyoto, Japan, September 2002.
8. Hummel, S., Frisbee Flight Simulation and Throw Biomechanics, MS Thesis, UC Davis, 2003
9. Spencer J et al, Mars Pathfinder Entry and Descent Analysis, Journal of Spacecraft and Rockets, 1999.
10. Paetzold, M., Bird, M. K., Volland, H. 1991. GIOTTO-Halley encounter - When was the large nutation generated?. Astronomy and Astrophysics 244, L17-L20